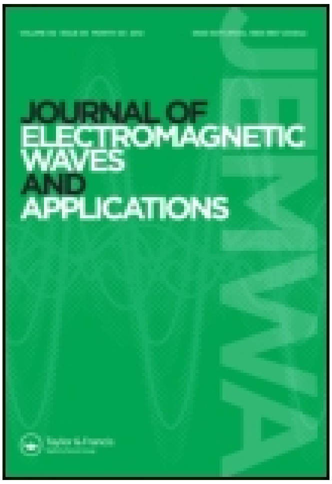

Journal of Electromagnetic Waves and Applications
Publication details, including instructions for authors and subscription information:
http://www.tandfonline.com/loi/tewa20

Dual-band bandpass filter with independent passbands using resonant junctions

Jose-Luis Olvera-Cervantes[a] & Alonso Corona-Chavez[a]
[a] Electronics Department, National Institute of Astrophysics, Optics and Electronics (INAOE), Puebla, Mexico

Published online: 04 Aug 2015.

Journal of Electromagnetic Waves and Applications, 2015
Vol. 29, No. 14, 1935–1941, http://dx.doi.org/10.1080/09205071.2015.1067648

Taylor & Francis
Taylor & Francis Group

Dual-band bandpass filter with independent passbands using resonant junctions

Jose-Luis Olvera-Cervantes* and Alonso Corona-Chavez

Electronics Department, National Institute of Astrophysics, Optics and Electronics (INAOE), Puebla, Mexico

(*Received 19 May 2015; accepted 24 June 2015*)

This document presents a dual-band bandpass filter with fully independent passbands. The filter is based on a novel dual-band resonant junction (DBRJ) and $\lambda/2$ resonators. This approach allows different filter order at each passband, independent fractional bandwidth tuning, and independent filter response at each band. The DBRJs consist of a short-circuited quarter-wavelength resonator. One prototype is presented with Butterworth and Chebyshev responses and center frequencies at 1.8 and 2.45 GHz.

Keywords: dual-band filters; resonant junction; microstrip filters; microwave resonators

1. Introduction

Dual-band bandpass filters are components accomplishing the filtering function at two different frequencies. Due to the rapid development of wireless technologies, dual-band microwave filters have become an attractive component for reducing system complexity and cost. Dual-band bandpass filters may be designed using: (a) double-sided parallel-strip lines,[1] (b) modified resonators including stepped impedance resonators (SIRs),[2] stub-loaded open-loop resonators, or split-ring resonators,[3] (c) CRLH metamaterial transmission lines,[4] and (d) the combination of two individual bandpass filters.[5,6]

The combination of two individual bandpass filters may be realized using the conventional diplexer approach, [5] where fully independent passbands may be obtained but it is well known that the filter size increases due to the impedance matching networks. Another option is to use dual-feeding structures as in [6], where input/output coupling structures based on SIRs are used to combine two passband filters. However, in this technique, both bandwidths cannot be tuned independently as the external quality factors are interdependent. In addition, the number of poles at both passbands and the filter response has to be same for both bands.

The motivation of the present work is to have a dual-band bandpass filter with fully independent passbands. This involves freedom on the number of poles for each passband, independent tuning for each band, as well as independence on the filter response type. Moreover, no extra matching networks are required.

*Corresponding author. Email: jolvera@inaoep.mx

2. Proposed filter

Figure 1 shows the layout of the proposed dual-band filter designed on a Rogers 4003C with 1.524 mm thickness and design permittivity 3.5. The first passband has Butterworth response, FBW = 12.3%, four poles, and center frequency at f_1 = 1.8 GHz. The second passband exhibits Chebyshev response, FBW = 7.1%, 0.1 of ripple, three poles, and center frequency at f_2 = 2.45 GHz. The design parameters are [7]: $Q_{eiI} = Q_{eoI} = 6.22$, $K_{12I} = K_{34I} = 0.103$, and $K_{23I} = 0.066$ for the first passband and $Q_{eiII} = Q_{eoII} = 14.529$ and $K_{12II} = K_{23II} = 0.065$ for the second passband, where Q_{ein} and Q_{eon} are the input and output external quality factors at each passband n = {I, II}, and K_{ijn} is the mutual coupling coefficients between adjacent resonators of each filter.

The filter uses a dual-band resonant junction (DBRJ) at the input and output. The DBRJs consist of a short-circuited quarter-wavelength resonator and one half-wavelength resonator with fundamental resonances at f_1 = 1.8 GHz and f_2 = 2.45 GHz, respectively. The first passband is formed by the input DBRJ, two half-wavelength resonators (r2 and r3) at 1.8 GHz, and the output DBRJ. The second passband is created by coupling the input DBRJ with a half-wavelength resonator (R2) at 2.45 GHz, and the output DBRJ.

2.1. Design of the DBRJ

The resonant junction is designed to satisfy simultaneously the external quality factors which depend on the separation G and the position t of a microstrip line with width of wt = 3.0 mm used to attach SMA connectors. Figure 2 shows the resonant junction and a typical group delay response calculated from the S_{11} parameter. From the group delay, the resonant frequencies are verified at 1.8 and 2.45 GHz. It is important to note that the two resonant frequencies must be verified every time that the G and t are varied and the resonators must be tuned with the group delay to guarantee the two frequencies. Thus, Figure 2 is used to guarantee resonances at the desired passband and calculate external

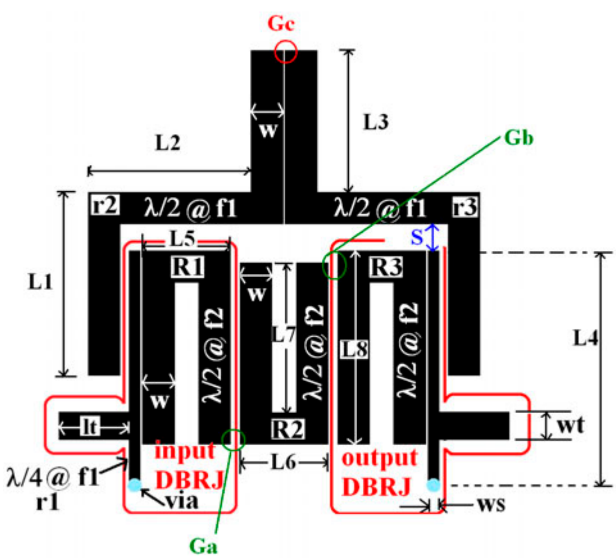

Figure 1. Layout of proposed filter.

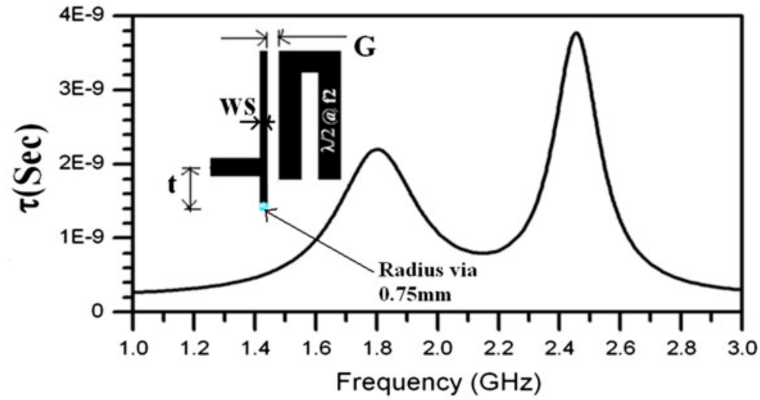

Figure 2. S_{11} group delay of the resonant junction.

quality factors at 1.8 and 2.45 GHz which are calculated with (1) and (2), respectively, where $\tau(f_i)$ is the group delay at each center frequency. Figure 3 shows a plot of the external quality factor Q_{eiI} vs. the tap position t for different gaps (G). From this plot, the required value tap position at 1.8 GHz is $t = 6.490$ mm for $Q_{eiI} = 6.22$. Also, it can be seen that the external quality factor at 1.8 GHz is almost independent on the separation G.

In a similar way, the external quality factor at 2.45 GHz is calculated considering the tap coupling $t = 6.490$ mm and different gap separation values. Figure 4 shows a plot of Q_{eiI} and Q_{eiII} vs. the gap separation G. This figure shows again that the gap separation modifies the external coupling at 2.45 GHz but the external quality factor is almost constant at 1.8 GHz. It is worthy to mention that results in Figures 3 and 4 were obtained changing t and G and adjusting the dimensions of resonator r1 and resonator R1 in order to assure resonances at 1.8 and 2.45 GHz.

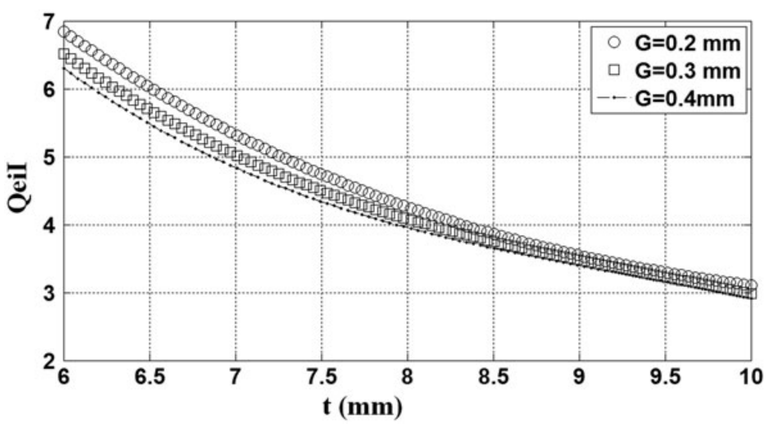

Figure 3. External quality factor at 1.8 GHz.

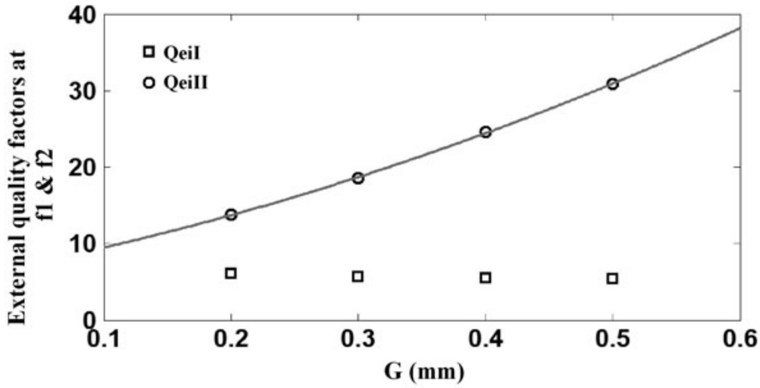

Figure 4. External quality factor at 2.45 GHz.

This independence is particularly important when designing dual-band filters since both external quality factors are not dependent on the filter order overcoming the problem with the structure in [6]. Thus, from Figure 4 the G value is 0.200 mm.

$$Q_{\mathrm{eiI}} = Q_{\mathrm{eoI}} = 2\pi f_1 \tau(f_1)/4 \tag{1}$$

$$Q_{\mathrm{eiII}} = Q_{\mathrm{eoII}} = 2\pi f_2 \tau(f_2)/4 \tag{2}$$

2.2. *Design of the second passband*

The second passband is created by coupling the input DBRJ with the half-wavelength resonator R2, and the output DBRJ. This passband requires input and output external quality factor values to be 14.529 and mutual couplings $K_{12\mathrm{II}} = K_{23\mathrm{II}} = 0.065$. The quality factors are achieved with the resonant junction previously described. The mutual coupling coefficient $K_{12\mathrm{II}}$ is related to separation G_{a} between the input DBRJ and the resonator R2. For different G_{a} values, the mutual coupling coefficient $K_{12\mathrm{II}}$ is calculated values with (3) where the frequency of the upper peak f_{u} and the frequency of the lower peak f_{l} are obtained from a smooth $|S_{21}|$ curve with double-peak response as explained in [8]. Because $K_{34\mathrm{II}} = K_{12\mathrm{II}} = 0.065$ then the gap separation between resonator $R2$ and the output DBRJ is $G_{\mathrm{b}} = G_{\mathrm{a}} = 1.20$ mm, a plot of K_{12} vs. the separation G_{a}.

$$K_{ij} = \frac{f_{\mathrm{u}}^2 - f_{\mathrm{l}}^2}{f_{\mathrm{u}}^2 + f_{\mathrm{l}}^2} \tag{3}$$

2.3. *Design of the first passband*

The first passband is formed by coupling the input resonant junction with the two half-wavelength resonators r2 and r3, and the output DBRJ as shown in Figure 1. This passband requires external quality factor values to be 6.22 which are achieved with the same resonant junction.

The required mutual coupling coefficients for this passband are $K_{23I} = 0.066$ and $K_{12I} = K_{34I} = 0.103$. The mutual coupling coefficient K_{23I} is related to the separation G_C between resonator r2 and resonator r3. For different G_C values, the mutual coupling coefficient K_{23I} is calculated using (3). The required value is $G_C = 0.200$ mm.

In a similar way, the coefficient K_{12I} is calculated with (3) to different S values. The required value is $S = 3.570$ mm. Because $K_{12I} = K_{34I} = 0.103$ then the separation between resonator r3 and the output DBRJ is to be 3.57 mm. All dimensions were optimized in the simulator. The final dimensions are: $t = 6.490$, lt = 9.408 mm, $G = 0.200$ mm, G_a = Gb = 1.20, $G_c = 0.200$, $S = 3.57$ mm, $w = 3.4$ mm, $L1 = 18.9$ mm, $L2 = 17.21$ mm, $L3 = 15.33$ mm, $L4 = 25.2$ mm, $L5 = L6 = 9.3$ mm, $L7 = 15.980$, $L8 = 20.5$ mm, ws = 1.2 mm, and wt = 3 mm.

3. Simulated and experimental results

Figure 5 shows the fabricated filter. The circuit was fabricated using a PCB milling machine and measured with a two-port vector network analyzer. Figure 6 shows the simulated S-parameters from 1.45 to 3.0 GHz. The two passbands are centered at 1.8 and 2.45 GHz. The return losses are better than 20 dB in the passbands. The FBW in simulations is 12.31% for the first band and 7.343% for the second passband. Figure 7 shows the measured S-parameters for the same frequency range. In measurement, the two passbands are centered at 1.78 and 2.41 GHz. Return losses are better than 10 dB at each passband. Insertion losses are better than 1.8 and 1.4 dB for the first and second passband, respectively. The maximum attenuation between the two passbands is −24.8 dB. The measured FBW is 12% for the first band and 8.2% for the second passband. There are slight differences between the simulation and experimental results due to manufacturing errors and material tolerances.

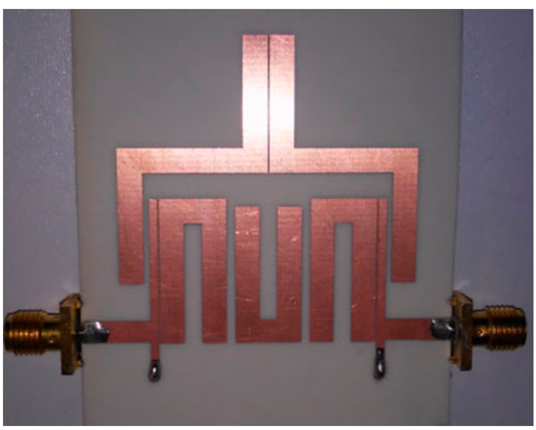

Figure 5. Fabricated filter.

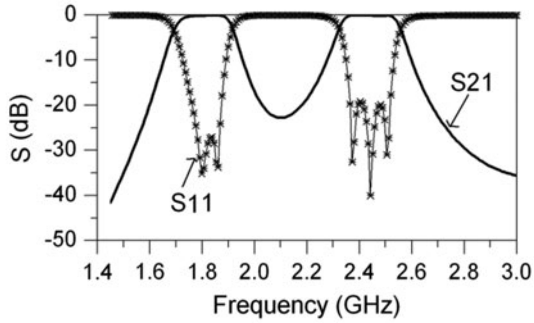

Figure 6. Simulated results.

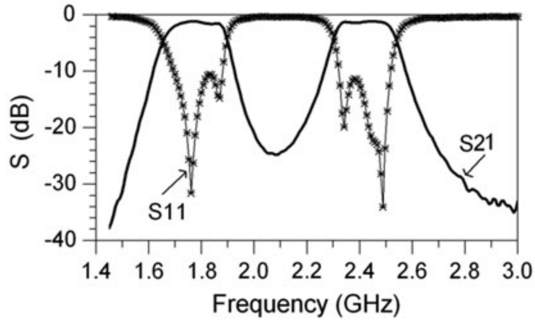

Figure 7. Experimental results.

4. Conclusions

In this paper, a new type of dual-band bandpass filter based on DBRJs and $\lambda/2$ resonators was presented. This filter has two passbands with center frequencies at 1.8 and 2.45 GHz. The new feeding DBRJs allow independent calculation of the external quality factors for each band, thus different FBWs can readily be designed. Good agreement between the simulation and measurement was achieved.

References

[1] Jiang W, Zhou L, Gao A-M, Shen W, Yin W-Y, Mao. Compact dual-mode dual-band balun filter using double-sided parallel-strip line. Electron. Lett. 2012;48:1351–1352.
[2] Zhang YP, Sun M. Dual-band microstrip bandpsss filter using stepped-impedance resonators with new coupling schemes. IEEE Trans. Microwave Theory Tech. 2006;54:3779–3785.
[3] Li M-H, Yang H-L, Lin H, Xiao B-X. Compact dual-band band-reject filter using complementary split-ring resonators. Electron. Lett. 2012;48:574–575.
[4] Tseng C-H, Itoh T. Dual-band bandpass and bandstop filters using composite right/left-handed metamaterial transmission lines. IEEE MTT-S Int. Dig. 2006;1:931–934.
[5] Miyake H, Kitazawa S, Ishizaki T, Yamada T, Nagatow Y. A miniaturized monolithic dual band filter using ceramic lamination technique for dual mode portable telephones. IEEE MTT-S Int. Dig. 1997;1:789–792.
[6] Chen Ch-F, Huang T-Y, Wu R-B. design of dual- and triple-passband filters using alternately cascaded multiband resonators. IEEE Trans. Microwave Theory Tech. 2006;54:3550–3558.

[7] Hong J-S, Lancaster MJ. Microstrip filters for rf/microwave applications. New York (NY): Wiley; 2001.
[8] Swanson DG Jr. Narrow-band microwave filter design. IEEE Microwave Mag. 2007;8: 105–114.